

THE UNIVERSITY OF MICHIGAN  
COLLEGE OF ENGINEERING  
Department of Engineering Mechanics  
Department of Mechanical Engineering  
Tire and Suspension Systems Research Group

Technical Report No. 27

FORE-AND-AFT STIFFNESS CHARACTERISTICS OF PNEUMATIC TIRES

R. N. Dodge  
David Orne  
S. K. Clark

ORA Project 02957

administered through:

OFFICE OF RESEARCH ADMINISTRATION

ANN ARBOR

November 1966

en 8m

UMR 651

The Tire and Suspension Systems Research Group  
at The University of Michigan is sponsored by:

FIRESTONE TIRE AND RUBBER COMPANY

GENERAL TIRE AND RUBBER COMPANY

B. F. GOODRICH TIRE COMPANY

GOODYEAR TIRE AND RUBBER COMPANY

UNITED STATES RUBBER COMPANY



## TABLE OF CONTENTS

	Page
LIST OF ILLUSTRATIONS	vii
I. INTRODUCTION	1
II. SUMMARY	3
III. ANALYSIS	4
IV. COMPARISON OF THEORY WITH EXPERIMENT	11
V. ACKNOWLEDGMENTS	21
VI. REFERENCES	22
VII. DISTRIBUTION LIST	23



## LIST OF ILLUSTRATIONS

Table	Page
I. Summary of Geometric, Elastic, and Structural Properties of Five Automotive Tires	13
II. Summary of Experimental and Calculated Values of $K_F$	13
Figure	
1. Idealized model of pneumatic tire for analyzing fore-and-aft spring rates.	4
2. Loaded element of the elastic bar portion of the model.	5
3. Meridional cross-section of the tire.	8
4. Experimental apparatus for checking $K_S$ .	9
5. Load-deflection data for double tube experiment used to confirm the expression for $K_S$ .	10
6. Idealized mid-line profiles of five pneumatic tires.	12
7. Photograph of experimental apparatus for $K_F$ .	14
8. Schematic of fore-and-aft spring-rate test.	14
9. Fore-and-aft load-deflection curves. Tire No. 1.	15
10. Fore-and-aft load-deflection curves. Tire No. 2.	16
11. Fore-and-aft load-deflection curves. Tire No. 3.	17
12. Fore-and-aft load-deflection curves. Tire No. 4.	18
13. Fore-and-aft load-deflection curves. Tire No. 5.	19

## I. INTRODUCTION

Pneumatic tires are functional parts of many operating mechanisms. In order to effectively design and engineer such mechanisms, it is often necessary to know the mechanical properties of the component parts, including the tires. One of the major roles of the Tire and Suspension Systems Research Group has been to study and analyze some of the important mechanical properties of pneumatic tires and to present rational methods for predicting them.

For the past several years an extensive structural analysis of the tire treated as a nonisotropic toroidal shell has been pursued. This has been a large undertaking and, although not complete, is slowly becoming usable. The analysis for the axisymmetric inflation problem currently provides good numerical results, and the analysis for the static loaded tire shows considerable promise of being equally useful. However, these analyses require a great deal of understanding and practice on the part of the user before practical results can be gotten from them. Thus, even though such analyses will eventually be available for more complete understanding of the pneumatic tire's role as an elastic body, less complicated methods for estimating important mechanical properties of tires are highly desirable.

Several paths have been followed by this research group in developing methods for predicting mechanical properties of tires. One technique involved modeling of the pneumatic tire as a cylindrical shell supported by an elastic foundation.<sup>5-7</sup> This model provides relations for predicting several properties involving deformation in the plane of the wheel, such as patch length



vs. vertical deflection, vertical load vs. vertical deflection, plane vibration characteristics, transmissability characteristics, and dynamic response to a point load.

A more recent attempt<sup>4</sup> involved analyzing the pneumatic tire as a string on an elastic foundation. This model is primarily used to predict lateral stiffness characteristics, vertical stiffness characteristics and twisting moments. However, this model has been found to be useful only when the inflation pressure is high, such as in the case of aircraft tires.

This report presents a method for predicting the fore-and-aft stiffness characteristics of pneumatic tires. Fore-and-aft properties are important in the overall analysis of a tire since they represent the contributions of the carcass and tread to braking and tractive elasticity. A different model is required here since the cylindrical shell and the string on the elastic foundation do not provide means for transmitting such loads. It is hoped that this model will prove satisfactory for predicting fore-and-aft characteristics of various tire designs.

## II. SUMMARY

An elastic bar supported by a foundation exhibiting elasticity in shear serves as a model for determining the fore-and-aft stiffness properties of a pneumatic tire. The differential equation representing the deformation is derived and solved, and the resulting solution serves as a means for calculating a fore-and-aft spring rate for the model.

A series of five tires of various sizes and structures was used for testing the validity of the proposed model. A set of static tests was performed to establish an experimental value for the fore-and-aft spring-rate for the various tires. Additional structural data, required by the analytical solution of the model, were also obtained from the tires. A comparison of the calculated and experimental results was reasonably satisfactory, indicating that the proposed model can be used to roughly approximate fore-and-aft stiffness characteristics.

A complete tabular summary of the geometry and composition of the five tires is included for easy reference. All experimental and analytical results are summarized and compared in graphical form.

### III. ANALYSIS

To represent fore-and-aft stiffness characteristics, the pneumatic tire is idealized as an elastic bar supported by an elastic shear foundation (see Figure 1). The elastic bar portion of the model represents the tread region of the tire which is loaded by the fore-and-aft load  $F$ . In addition to the restraint offered by the stiffness of the tread region itself, resistance to deformation by the load  $F$  is provided by the tires' ability to withstand shearing forces in the sidewall regions. This portion of the tire is represented in the model by the elastic shear foundation.

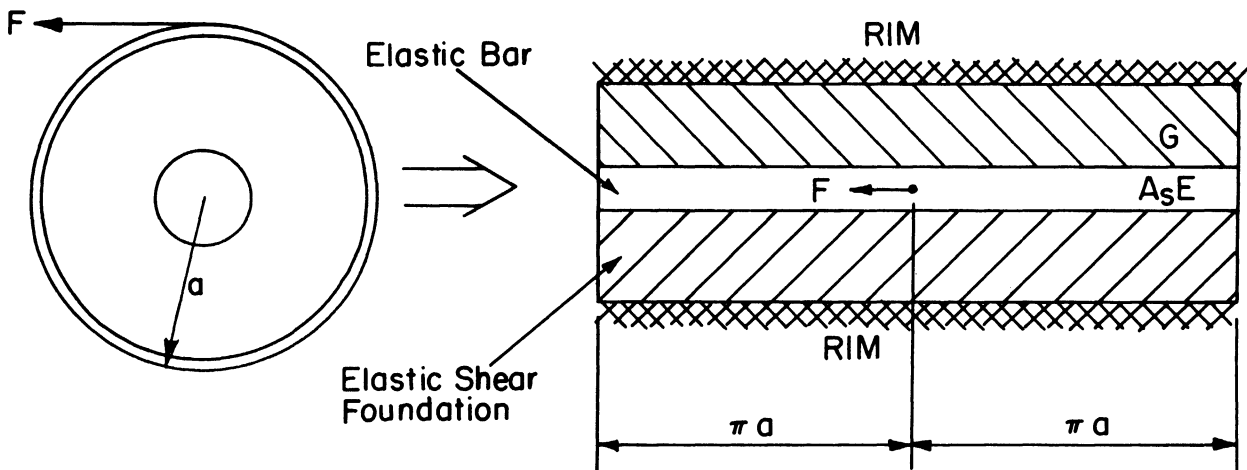


Figure 1. Idealized model of pneumatic tire for analyzing fore-and-aft spring rates.

If it is assumed that the restraining force of the elastic shear foundation is directly proportional to the displacement, an elemental segment of the elastic bar can be set in equilibrium as shown in Figure 2. Note that ad-

vantage is taken of the symmetry present in the model.

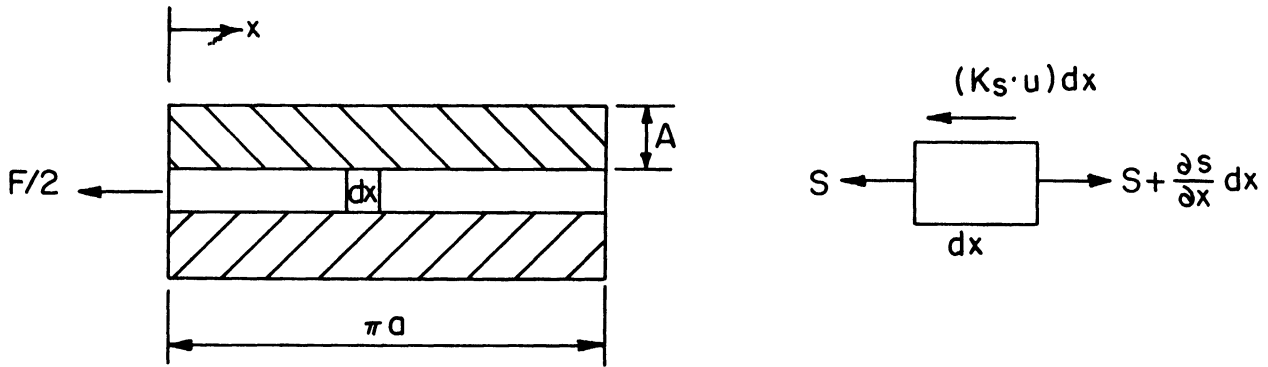


Figure 2. Loaded element of the elastic bar portion of the model.

In Figure 2,  $S$  is the force acting on the bar,  $u$  is the displacement, and  $K_s$  is the spring rate per unit length of the shear foundation. It is assumed that  $K_s$  is provided only by the shear resistance of the sidewall. From Figure 2, it is seen that one may approximate

$$K_s = \frac{2GH}{A}$$

where  $G$  is the effective shear modulus of the sidewall,  $H$  is the sidewall thickness, and  $A$  is the length along the sidewall from the rim to the point of intersection of the tread and carcass.

From equilibrium of the element,

$$\frac{\partial S}{\partial x} - K_s u = 0$$

$$S = TA_s = EeA_s = A_s E \frac{\partial u}{\partial x}$$

where  $T$  is the stress,  $e$  the resulting strain,  $A_s$  the cross-sectional area of the bar at any location, and  $E$  the effective extension modulus of the tread region in the circumferential direction, Thus,

$$\frac{\partial^2 u}{\partial x^2} - q^2 u = 0 \quad (1)$$

where

$$q^2 = \frac{K_s}{A_s E}$$

The general solution of this equation is

$$u = C_1 \cosh qx + C_2 \sinh qx \quad (2)$$

The boundary conditions for this problem are

$$\text{at } x = 0, \quad S = \frac{F}{2} \quad (3)$$

$$\text{at } x = \pi a, \quad S = 0$$

Substituting (3) into (2) gives

$$C_1 = \frac{-F}{2A_s E \tanh \pi a q}; \quad C_2 = \frac{F}{2A_s E q} \quad (4)$$

Thus,

$$u(x) = \frac{F}{2A_s E q} \left[ \sinh qx - \frac{\cosh qx}{\tanh q\pi a} \right] \quad (5)$$

The fore-and-aft stiffness is determined by finding the ratio of the applied load to the displacement at the point of application of the load. Thus,

$$K_f = \left| \frac{F}{u(0)} \right| = \left| - 2A_s E q (\tanh q \pi a) \right| \quad (6)$$

Equation (6) now represents a relationship for the fore-and-aft spring-rate of a pneumatic tire idealized as an elastic bar supported by a shear foundation. As can be seen From Eqs. (1) and (6), the application of Eq. (6) to a real tire requires a knowledge of the effective stiffness of the tread region in the circumferential direction  $A_s E$ , the effective shear modulus of the sidewall region  $G$ , the effective sidewall thickness  $H$ , and the length along the mean meridional section from the rim to the intersection of the tread and carcass,  $A$ .

The extension modulus in the circumferential direction and the shear modulus of the carcass usually vary from one location to another in the meridional direction because of the orthotropic nature of the tire carcass, so some averaging criteria must be established in order to compute  $A_s E$  and  $G$  for a given tire section. Such a criteria can be established by referring to Figure 3 and defining the effective  $A_s E$  and  $G$  by:

$$(A_s E)_{\text{eff.}} = \frac{\int_0^{\phi_i} (A_s E) d\phi}{\int_0^{\phi_i} d\phi} = \frac{\int_0^{\phi_i} \left[ E_{\theta} \left( h_c + h_t \frac{E_t}{E_{\theta}} \right) \right] d\phi}{\int_0^{\phi_i} d\phi} \quad (7)$$

$$G_{\text{eff.}} = \frac{\int_{\phi_i}^{\phi_r} G_{12} d\phi}{\int_{\phi_i}^{\phi_r} d\phi}$$

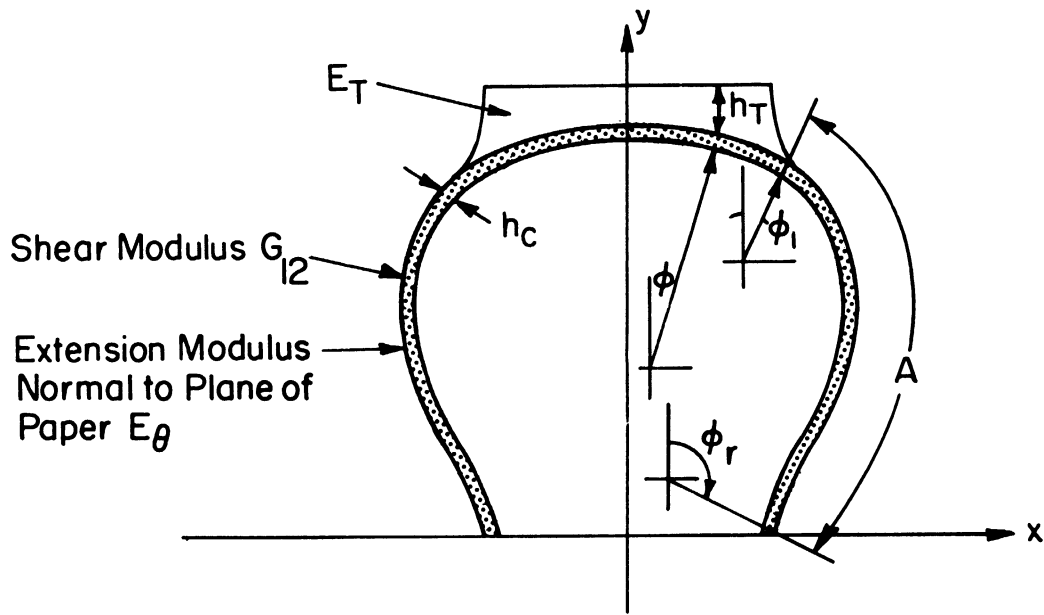


Figure 3. Meridional cross-section of the tire.

In Eqs. (7),  $\phi$  is the location angle in the meridional plane,  $E_\theta$  is the extension modulus in the circumferential direction,  $h_c$  is the effective thickness of carcass at any location,  $h_t$  is the effective tread thickness at any section,  $E_t$  is the Young's modulus of the tread stock, and  $G_{12}$  is the effective shear modulus of the carcass at any location. Using References 1 and 2 as a guide,  $E_\theta$  and  $G_{12}$  can be calculated for any meridional location knowing only certain elastic and geometric parameters required by most tire designers.

In order to establish some validity for the assumption that the shear foundation modulus  $K_s$  can be estimated by considering shear effects only, a simple experiment was performed by gluing a metal strip along the line of contact of two rubber cylinders placed side by side (see Figure 4). A load was attached to the bar and the resulting deflection was measured by the dial in-

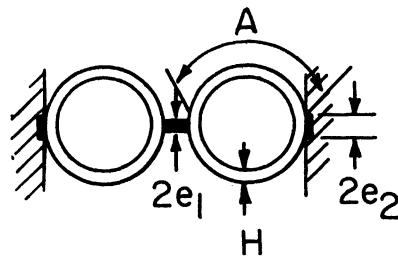
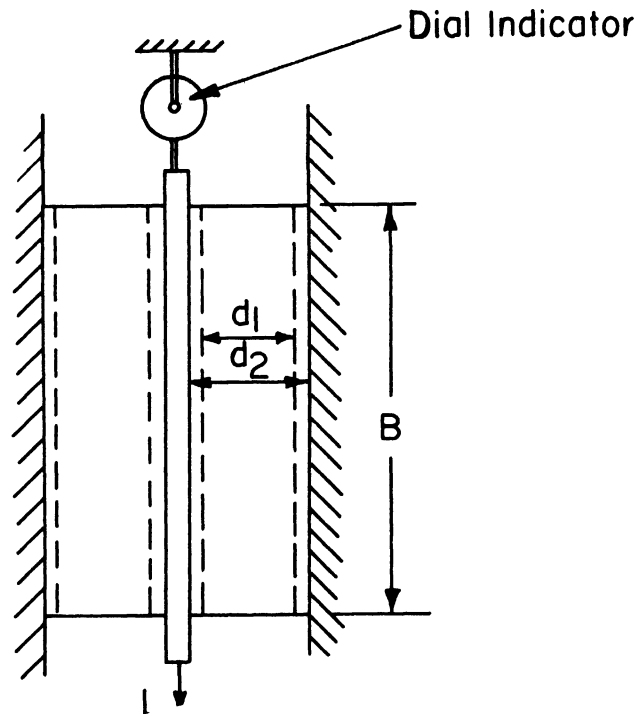


Figure 4. Experimental apparatus for checking  $K_S$ .

indicator. The slope of the experimental load-deflection curve, related to  $K_S$ , was then compared with the value of  $K_S$  obtained from the relation given above,

$$K_S = \frac{2GH}{A}$$

A summary of this experiment is presented below:

$$\begin{aligned} B &= 10.0 \text{ in.} & d_2 &= 1.252 \text{ in.} \\ d_1 &= 0.986 \text{ in.} & H &= 0.133 \text{ in.} \end{aligned}$$



$$e_1 = 0.10 \text{ in.}$$

$$A = 1.72 \text{ in.}$$

$$e_2 = 0.15 \text{ in.}$$

$$G = 200/3 \text{ lb/in.}^2$$

From the test data (Figure 5), the slope of the load-deflection curve yields a  $K_s = 22.0 \text{ lb/in./in.}$  The calculated value for the double tube is

$$K_s = \frac{4GH}{A} = \frac{4\left(\frac{200}{3}\right)(.133)}{1.72} = 20.6 \text{ lb/in./in.}$$

(A factor of 4 appears in this computation because of the double tube arrangement.) The close comparison between the experimental  $K_s$  and the calculated one, assuming that the foundation is flat rather than curved, indicates that any curvature effects are minor.

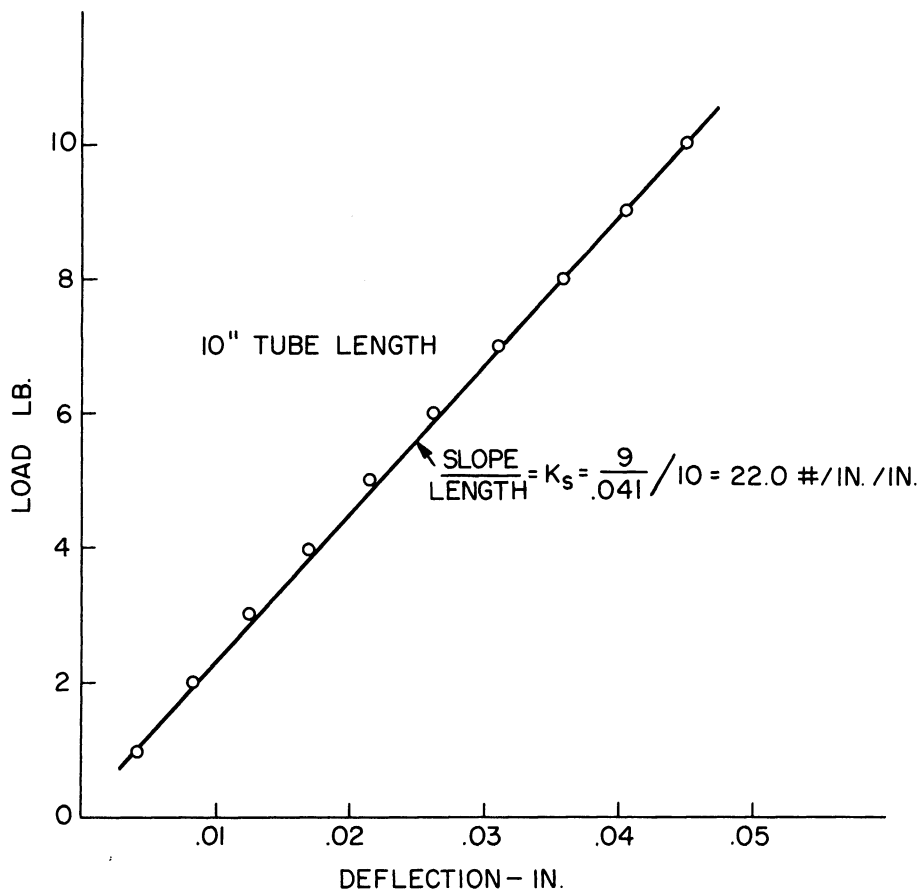


Figure 5. Load-deflection data for double tube experiment used to confirm the expression for  $K_s$ .

#### IV. COMPARISON OF THEORY WITH EXPERIMENT

In an attempt to investigate the applicability of Eq. (6), a series of static fore-and-aft stiffness tests were run on representative tires. Before reporting these tests and their results, the five tires used are described in detail. The idealized centerline profiles of the tires are shown in Figure 6. Tire No. 1 is a domestic 4-ply, 8.00 x 14 bias-ply tire with standard nylon cord. Tire No. 2 is a 2-ply, 7.50 x 14 bias-ply tire with standard nylon cord. Tire No. 3 is an imported 4-ply, 5.90 x 15 bias-ply tire with nylon cord. Tire No. 4 is an imported 7.50 x 14 radial-ply tire with overheads reinforced with wire cord. Tire No. 5 is a European made 155 mm x 15 in. radial-ply tire with overheads reinforced with nylon cord.

Table I is a summary of the pertinent elastic and geometric parameters required from the five tires. Using the results in this table, Figure 6, and Eqs. (6) and (7), it is possible to calculate the fore-and-aft stiffness of the five tires. Carrying out these computations gives the calculated values presented in Table II.

To check the accuracy of the calculated values, the five tires were tested in the apparatus illustrated in Figures 7 and 8. In this testing procedure the tires were loaded vertically to a fixed deflection. Then a varying fore-and-aft load was applied and the resulting deflection recorded. The slope of these load-deflection curves represents the experimental fore-and-aft spring-rates. These tests were run for different vertical deflections and inflation pressures. The results of these tests are summarized in Figures 9 through 13.

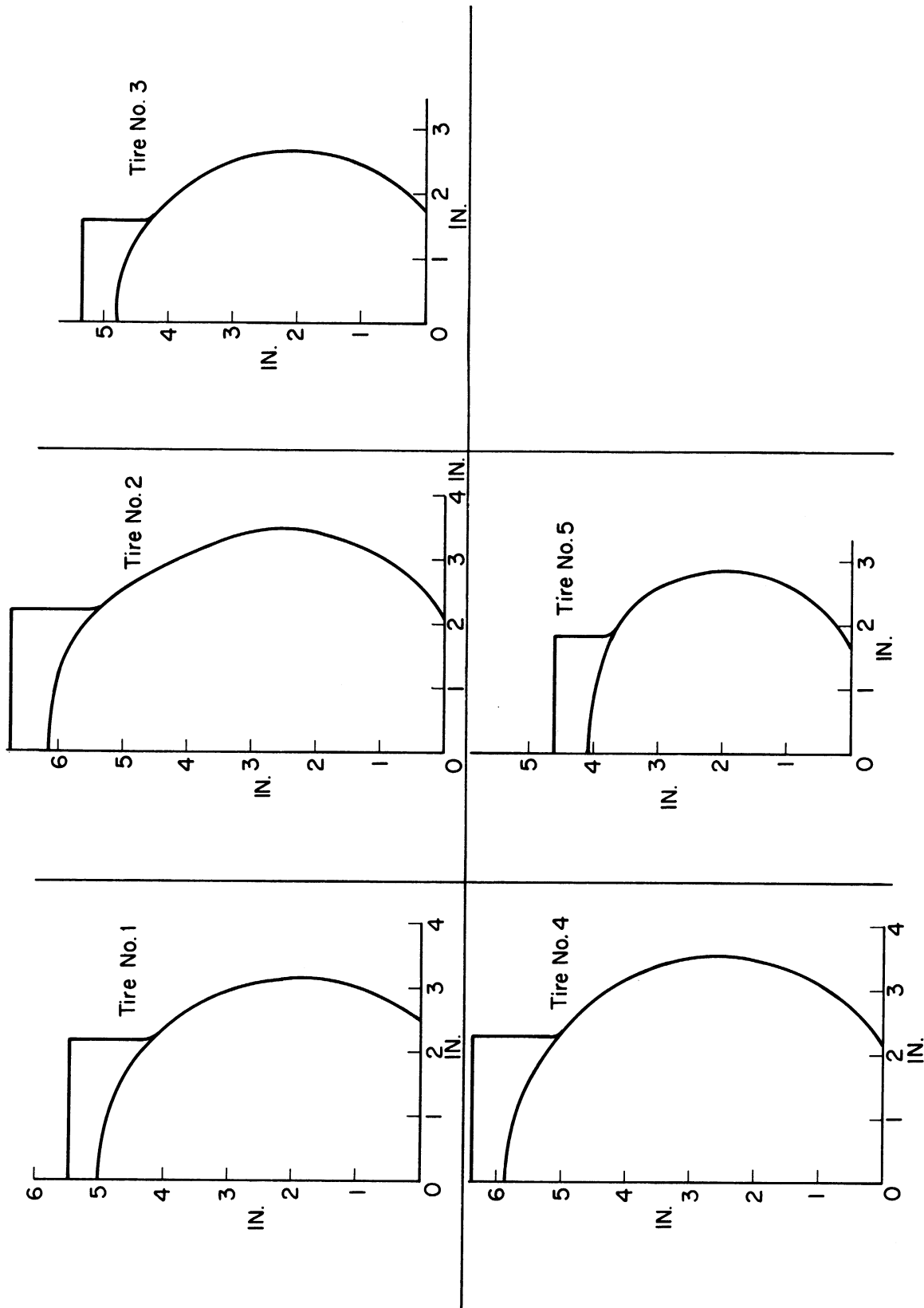


Figure 6. Idealized mid-line profiles of five pneumatic tires.

TABLE I

## SUMMARY OF GEOMETRIC, ELASTIC, AND STRUCTURAL PROPERTIES OF FIVE AUTOMOTIVE TIRES

Item (Ref. 5, Table I)	Tire 1		Tire 2		Tire 3		Tire 4		Tire 5	
	Bias-Ply 8.00x14	Bias-Ply 7.50x14	Bias-Ply 7.50x14	Bias-Ply 7.50x14	Bias-Ply 5.20x15	Bias-Ply 5.20x15	Radial-Ply 7.50x14	Radial-Ply 7.50x14	Radial-Ply 152mm x15	Radial-Ply 152mm x15
A0 - outside radius of tire	12.525	13.94	13.94	13.94	12.875	12.875	13.44	13.44	12.25	12.25
L - half circumference	39.35	43.79	43.79	43.79	40.45	40.45	42.22	42.22	38.48	38.48
ET - extension modulus, tread rubber	670.	560.	560.	560.	481.	481.	690.	690.	490.	490.
A - length, mean meridional section	4.6408	5.8404	5.8404	5.8404	4.9217	4.9217	5.7238	5.7238	4.5529	4.5529
H - effective thickness for $K_s$	0.164	0.220	0.220	0.220	0.160	0.160	0.250	0.250	0.280	0.280
G - effective shear modulus for $K_s$	28440.	47164.	47164.	47164.	43876.	43876.	269.	269.	144.	144.
$A_s^E$ - effective spring rate, circumferential	779.	747.	747.	747.	760.	760.	11906.	11906.	23027.	23027.
$K_s$ - spring rate, shear foundation	2010.	1747.	1747.	1747.	2852.	2852.	18.98	18.98	23.50	23.50
BETAC - cord half angle, crown	0.6458	0.6283	0.6283	0.6283	0.6109	0.6109	0.3142	0.3142	0.2356	0.2356
ROC - radial location, crown	12.120	13.38	13.38	13.38	12.355	12.355	12.92	12.92	11.70	11.70
ROB - radial location, rim	7.078	7.20	7.20	7.20	7.515	7.515	7.06	7.06	7.59	7.59
R - idealized radius, sidewall	3.22	3.03	3.03	3.03	2.84	2.84	3.13	3.13	2.17	2.17
$y_c$ - y-coordinate, center for R	1.935	2.490	2.490	2.490	2.092	2.092	2.454	2.454	1.939	1.939
$x_c$ - x-coordinate, center for R	-0.057	0.465	0.465	0.465	-0.146	-0.146	0.405	0.405	0.704	0.704
R1 - idealized radius, crown region	3.40	2.62	2.62	2.62	2.76	2.76	3.54	3.54	4.88	4.88
ERUB - extension modulus, carcass rubber	438.	310.	310.	310.	370.	370.	625.	625.	300.	300.
GRUB - shear modulus, carcass rubber	146.	103.	103.	103.	123.	123.	208.	208.	100.	100.
MURUB - Poisson ratio, carcass rubber	0.500	0.500	0.500	0.500	0.500	0.500	0.500	0.500	0.500	0.500
GCORR - shear modulus, cord	705.	705.	705.	705.	705.	705.	705.	705.	705.	705.
AESUBC - spring rate, cord	200.	623.	623.	623.	317.	317.	350.	350.	307.	307.
DIAMC - effective diameter, cord	0.025	0.040	0.040	0.040	0.026	0.026	0.025	0.025	0.023	0.023
MUC - Poisson ratio, cord	0.700	0.700	0.700	0.700	0.700	0.700	0.700	0.700	0.700	0.700
TPLY - effective ply thickness	0.041	0.055	0.055	0.055	0.040	0.040	0.040	0.040	0.040	0.040
NCORD - cord count, crown	26.	19.	19.	19.	24.	24.	18.	18.	20.	20.
ALFSTR - normal angle, intersection	0.7746	0.6085	0.6085	0.6085	0.6665	0.6665	0.6427	0.6427	0.5775	0.5775
ALPHR - normal angle, rim	2.2148	2.5331	2.5331	2.5331	2.3973	2.3973	2.4714	2.4714	2.6792	2.6792

TABLE II

SUMMARY OF EXPERIMENTAL AND CALCULATED VALUES OF  $K_f$ 

Tire	$K_f$ - lb/in.	
	Experimental	Calculated
1	2530	2503
2	2300	2286
3	2780	2944
4	1340	1469
5	1265	950

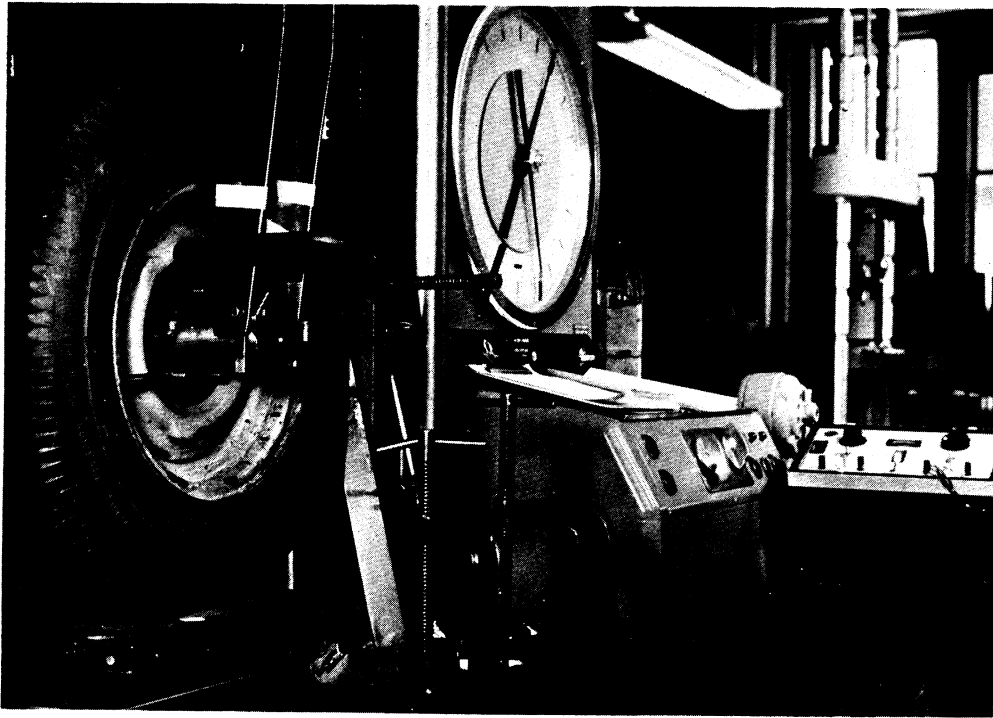


Figure 7. Photograph of experimental apparatus for  $K_f$ .

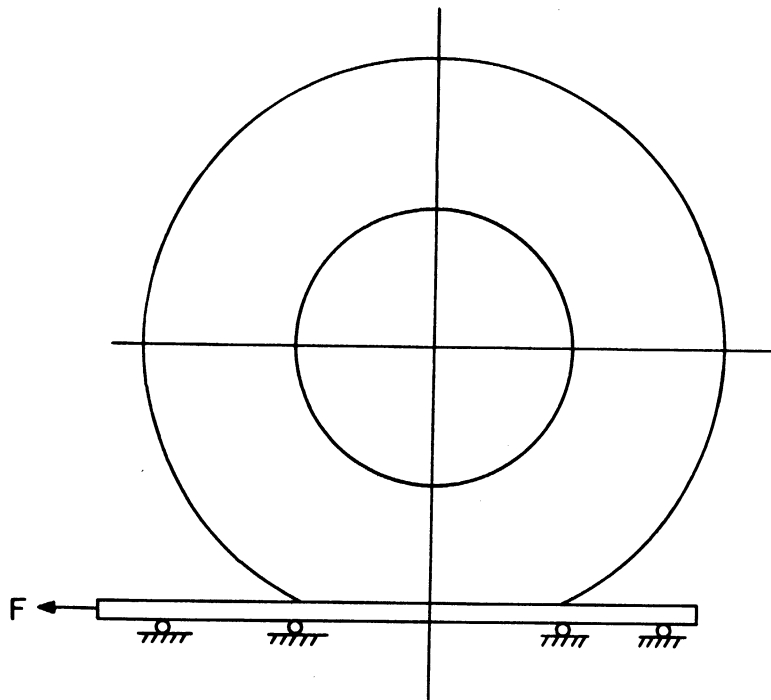


Figure 8. Schematic of fore-and-aft spring-rate test.

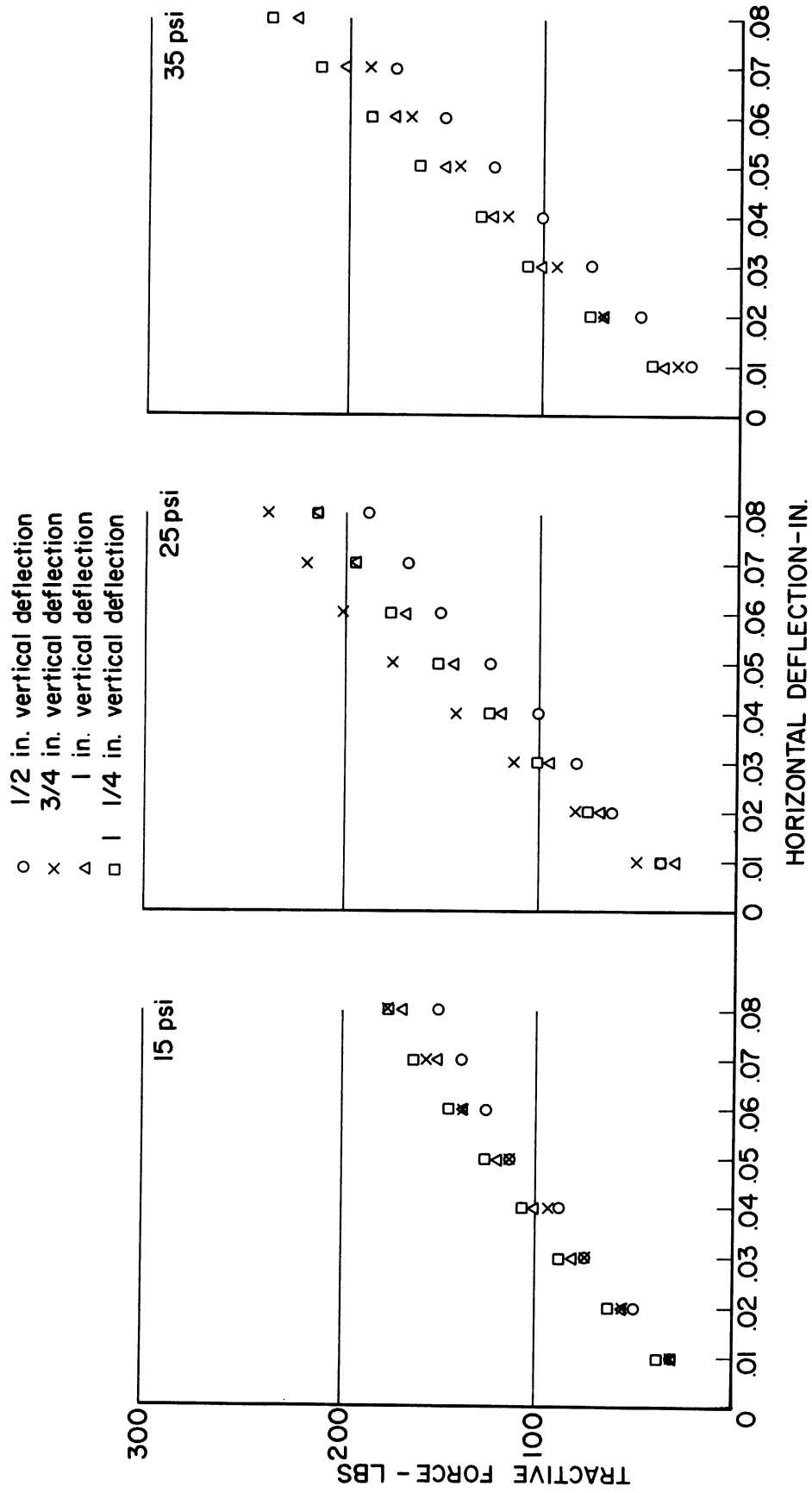


Figure 9. Fore-and-aft load-deflection curves. Tire No. 1.

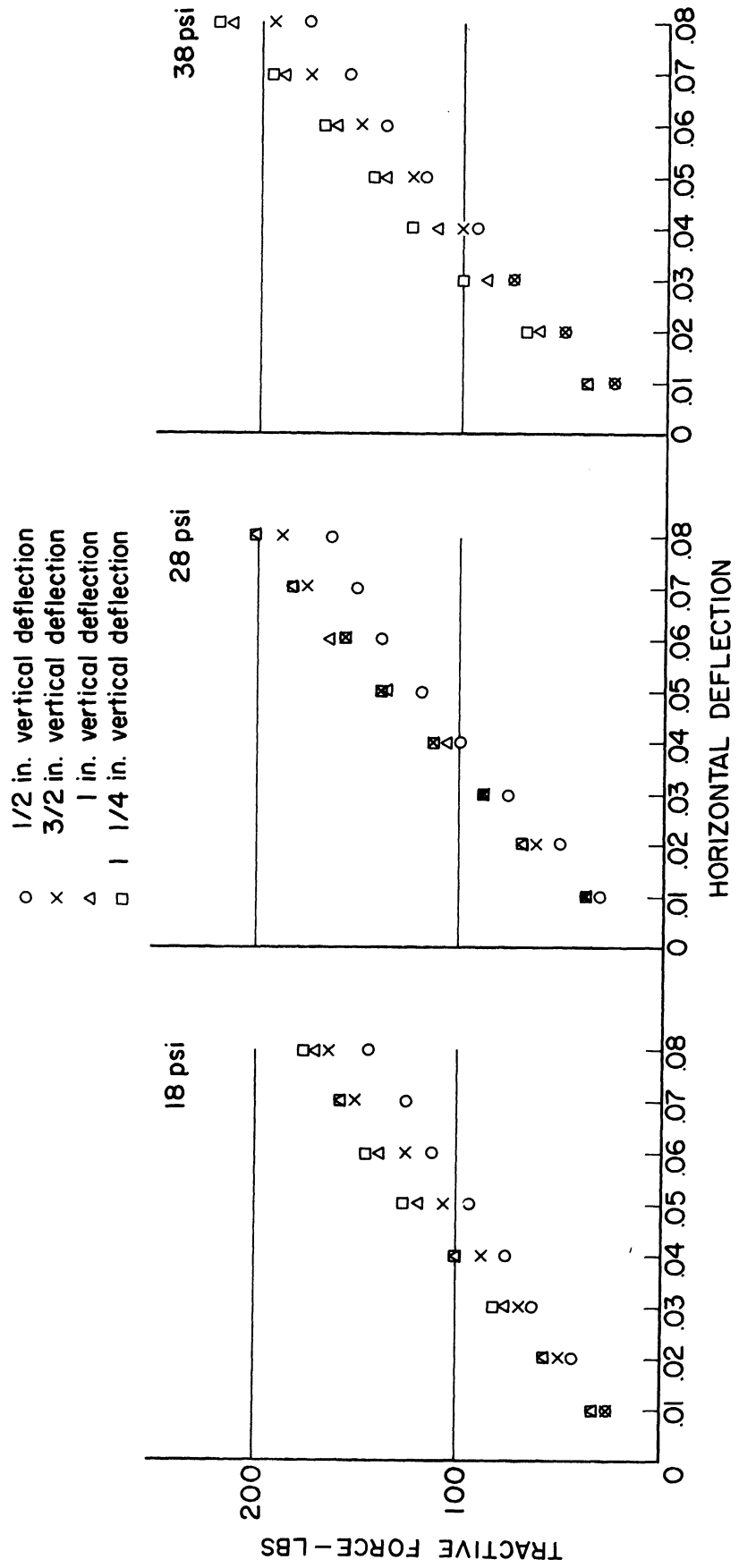


Figure 10. Fore-and-aft load-deflection curves. Tire No. 2.

- 1/2 in. vertical deflection
- × 3/4 in. vertical deflection
- △ 1 in. vertical deflection
- 1 1/4 in. vertical deflection

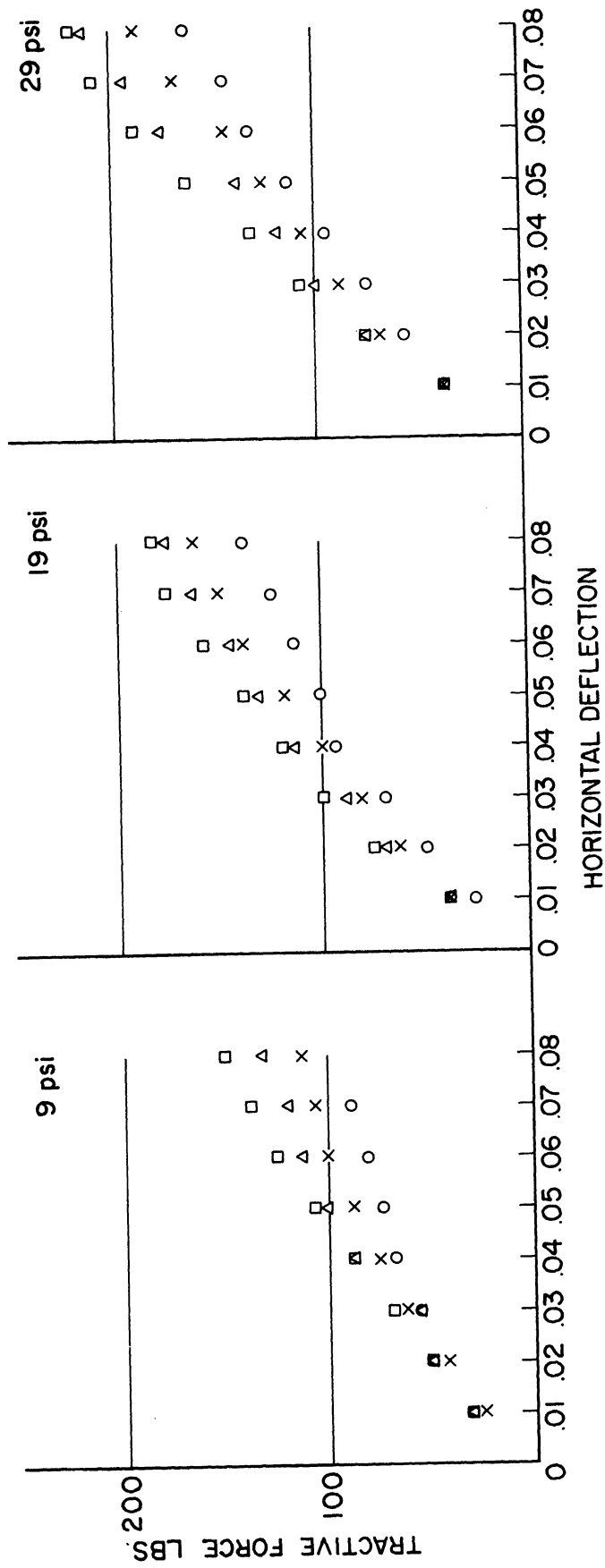


Figure 11. Fore-and-aft load-deflection curves. Tire No. 3.



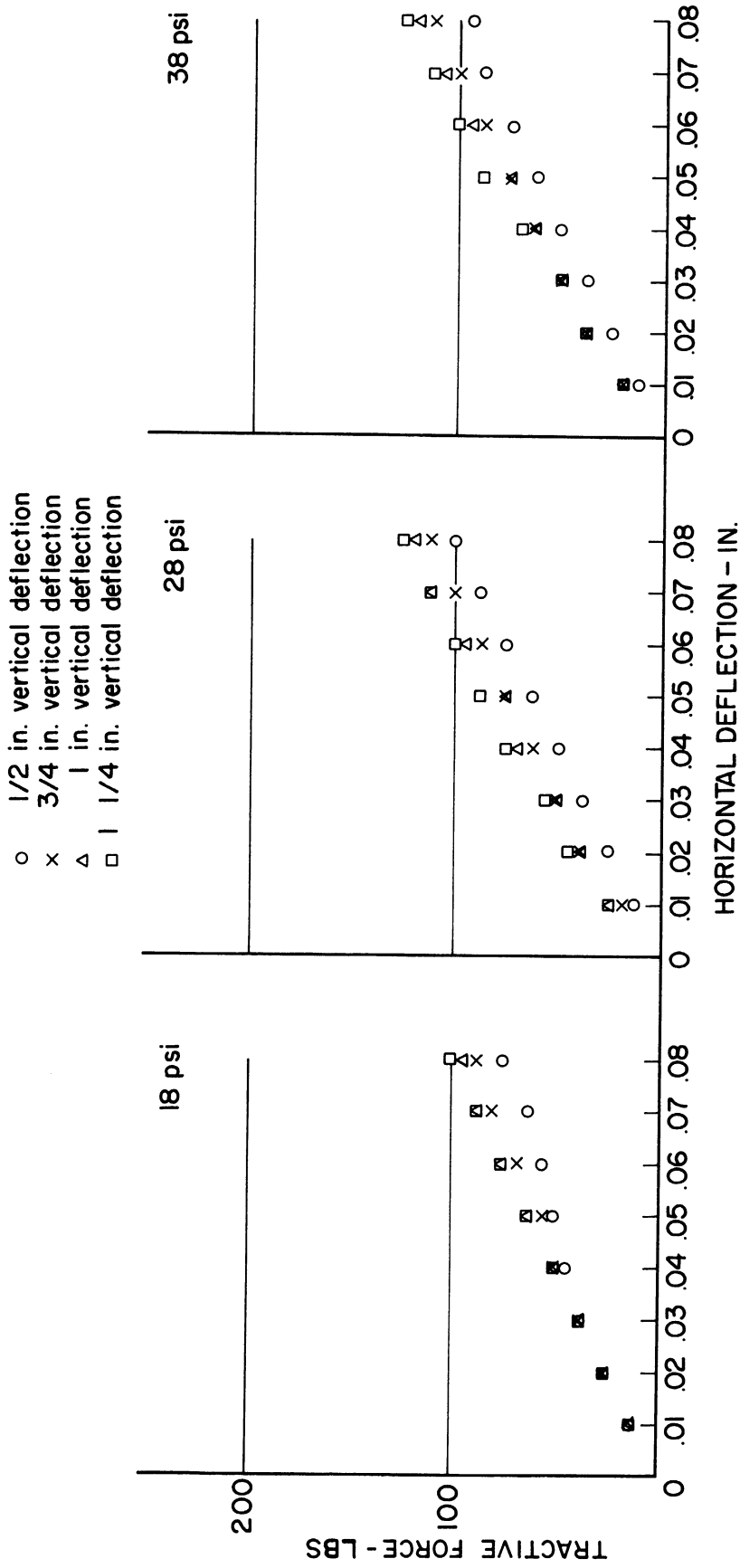


Figure 12. Fore-and-aft load-deflection curves. Tire No. 4.

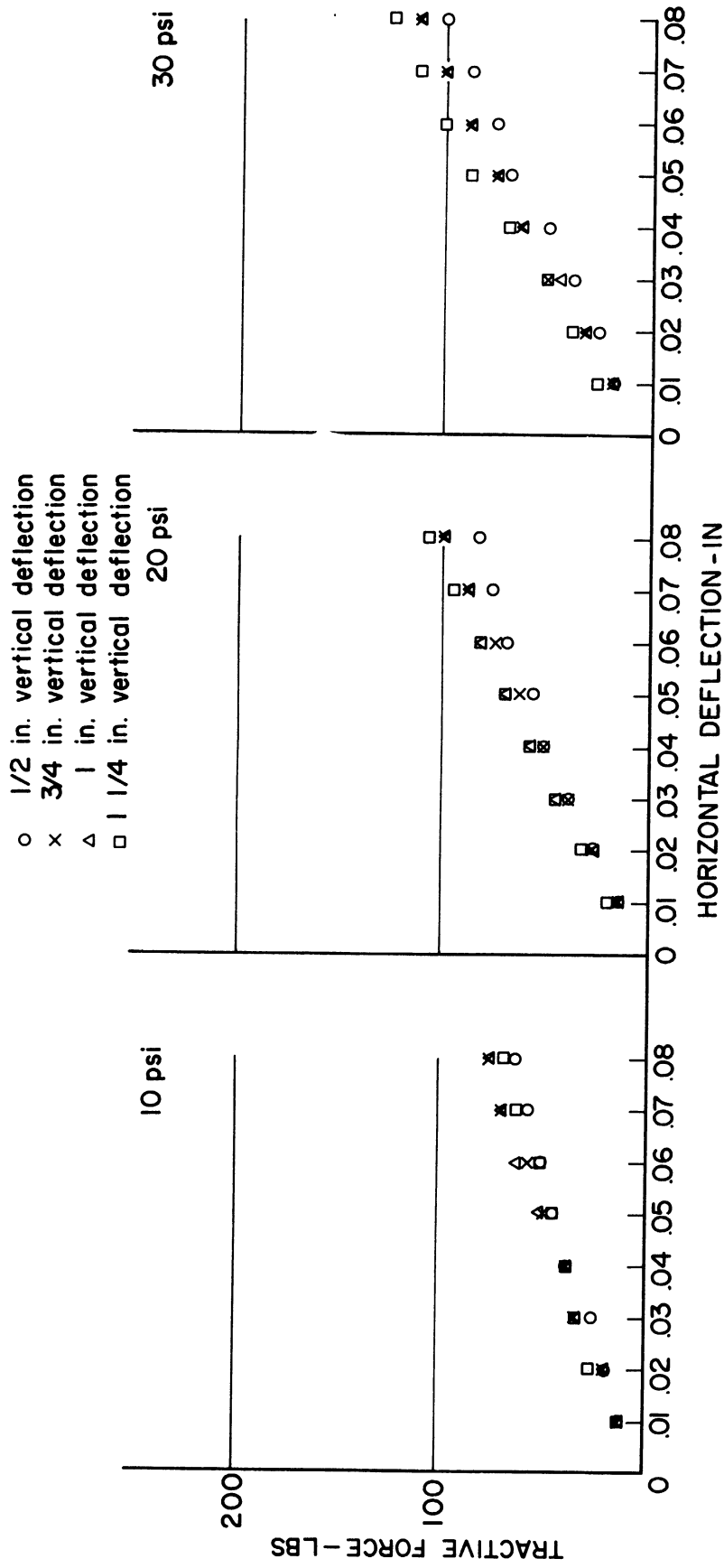


Figure 13. Fore-and-aft load-deflection curves. Tire No. 5.

In general it can be seen from these curves that the fore-and-aft spring-rate increases only slightly with increasing vertical load and with increasing internal pressure. Since Eq. (6) does not account for the slight increase due to these factors, a comparison between the experimental and calculated results must be made in a somewhat arbitrary fashion. However, since the experimental values are nearly the same for all conditions examined, any results used as a comparison with the calculated values will serve as a meaningful check. The comparisons shown in Table II are based on experimental values obtained from vertical tire deflections of one inch and by use of manufacturers rated inflation pressure. The experimental values were determined by measuring the slopes in the linear portions of the load-deflection curves. These comparisons indicate that the simple model formulated above gives a method for approximating the fore-and-aft spring-rate of pneumatic tires using only the geometric, elastic, and structural properties required by most tire designers.

## V. ACKNOWLEDGMENTS

The authors wish to thank Mr. B. Bourland, Mr. P. A. Schultz, and Mr. B. Bowman for their assistance in obtaining the experimental data presented in this report.

## VI. REFERENCES

1. Clark, S. K., "The Plane Elastic Characteristics of Cord-Rubber Laminates," The University of Michigan, ORA Technical Report 02957-3-T, October, 1960.
2. Clark, S. K., R. N. Dodge, N. L. Field, and B. Herzog, "Inflation of a Pneumatic Tire," The University of Michigan, ORA Technical Report 02957-14-T, February, 1962.
3. Smiley, R. F., and W. B. Horne, "Mechanical Properties of Pneumatic Tires with Special Reference to Modern Aircraft Tires," NACA Technical Note 4110, National Advisory Committee for Aeronautics, Washington, D.C., January, 1958.
4. Clark, S. K., "Simple Approximations for Force-Deflection Characteristics of Aircraft Tires," The University of Michigan, ORA Technical Report 05608-8-T, December, 1965.
5. Dodge, R. N., "Prediction of Pneumatic Tire Characteristics from a Cylindrical Shell Model," The University of Michigan, ORA Technical Report 02957-25-T, March, 1966.
6. Clark, S. K., "An Analog for the Static Loading of a Pneumatic Tire," The University of Michigan, ORA Technical Report 02957-19-T, March, 1964.
7. Tielking, J. T., "Plane Vibration Characteristics of a Pneumatic Tire Model," The University of Michigan, ORA Technical Report 02957-22-T, June, 1965.

VII. DISTRIBUTION LIST

	<u>No. of Copies</u>
The General Tire and Rubber Company Akron, Ohio	6
The Firestone Tire and Rubber Company Akron, Ohio	6
B. F. Goodrich Tire Company Akron, Ohio	6
Goodyear Tire and Rubber Company Akron, Ohio	6
United States Rubber Company Detroit, Michigan	6
The University of Michigan ORA File	1
S. K. Clark	1
Project File	10

UNIVERSITY OF MICHIGAN



3 9015 02539 7079